CompBat Deliverable

D3.1 Report on general isothermal cell modelling

Grant Agreement number	875565
Action Acronym	CompBat
Action Title	Computer aided design for next generation flow batteries
Funding Scheme	H2020-LC-BAT-2019
Duration of the project	36 months, 1 February 2020 – 31 January 2023
Work package	WP3 - *Stack and system modelling*
Due date of the deliverable	31 July 2021
Actual date of submission	30 September 2021
Lead beneficiary for the deliverable	SKOLTECH
Dissemination level of the deliverable	Public

Project coordinator's scientific representative

Dr. Pekka Peljo

Aalto korkeakoulusäätiö, Aalto University (Aalto), School of Chemical Engineering

Department of Chemistry and Materials Science

pekka.peljo@aalto.fi

CompBat project has received funding from the European Union's Horizon 2020 research and innovation programme under grant agreement No 875565. This document has been produced by the CompBat project. The content in this document represents the views of the authors, and the European Commission has no liability in respect of the content.

Authors		
Name	**Beneficiary**	**E-mail**
Keith Stevenson	SKOLTECH	k.stevenson@skoltech.ru
Mikhail Pugach	SKOLTECH	m.pugach@skoltech.ru
Aleksandr Kurilovich	SKOLTECH	a.kurilovich@skoltech.ru
Alexander Ryzhov	SKOLTECH	a.ryzhov@skoltech.ru
Gabriel Gonzalez	UTU	Gabriel.gonzalez@utu.fi

Internal QA			
Reviewer	**Date of review**	**Comments**	**Date of revision**
Pekka Peljo	30.09.2021	OK	

CompBat project has received funding from the European Union's Horizon 2020 research and innovation programme under grant agreement No 875565. This document has been produced by the CompBat project. The content in this document represents the views of the authors, and the European Commission has no liability in respect of the content.

Abstract/Executive summary

The report presents a single-cell zero-dimensional model for simulation of redox flow batteries with electrolytes based on the different redox-couples. The mathematical model has been generated within Task 3.1, and it represents deliverable D3.1 of the CompBat project.

The model is based on the approach for the determination of integral mass-transfer coefficient on the electrode-electrolyte interface that allows describing non-linear polarization behavior at high current densities. The kinetic parameters were also fitted for the effective single-step heterogeneous redox mechanisms at positive and negative electrodes in the case when activation losses treatment was needed to reproduce the experimental polarization curves. In addition, the model simulates the dynamic behavior of the cells working with different redox-couples in the wide range of loading current and electrolyte flow rates and thus allowing to explore their performance at different operating conditions. The influence of internal processes on the battery behavior has been analyzed and the effect of mass-transport limitations has been estimated. The key parameters (coulombic, voltage and energy efficiencies) of the batteries have been computed at least for 4 different current densities laid in the range of 20 – 150 mA cm^{-2}.

The developed model will be used as basis for non-isothermal model in Task 3.2 for simulation of redox flow battery dynamics. In addition, the results related to losses analysis will be used in Task 3.3 for simulation of shunt currents and in Task 3.5 for techno-economic studies.

CompBat project has received funding from the European Union's Horizon 2020 research and innovation programme under grant agreement No 875565. This document has been produced by the CompBat project. The content in this document represents the views of the authors, and the European Commission has no liability in respect of the content.

compbat

Contents

1 Introduction

The CompBat project aims at developing a set of tools for discovery of new prospective candidates for next generation of redox flow batteries (RFB). Mathematical modeling, that complements experimental testing, is a key tool that allows testing of particular candidates, including electrolytes, membranes and geometrical parameters, on a battery level at operating conditions that are close to operational. This development is carried out within work package WP3.

In the present WP we design isothermal zero-dimensional model of RFB that is based on a charge conservation and a set of voltage closures, including equilibrium potential, Nernst equation, Ohmic, concentration and activation losses. The model is able to accurately simulate RFB voltage and state of charge with high accuracy (average error of less than 5% on voltage) and allows real-time battery operation simulation. The model is scalable and will be extended with non-isothermal and shunt current effects later.

Herein, we report on a model basic assumptions and equations. We present simulation results for different electrolytes and losses analysis identifying the most important processes in the cell. In addition, we show the performance curves that can be used for simplified estimation of battery performance at different loading conditions.

2 Mathematical model

In the present WP we derive equations of charge conservation in two tanks and two cells, total of 8 variables – Vanadium ions or organic redox species concentrations, and impose

CompBat project has received funding from the European Union's Horizon 2020 research and innovation programme under grant agreement No 875565. This document has been produced by the CompBat project. The content in this document represents the views of the authors, and the European Commission has no liability in respect of the content.

closure for voltage calculations based on cell concentrations and current through the cell, that include equilibrium potential (zero-current 50% state of charge potential), Nernst equation, Ohmic, concentration and activation losses. The model is implemented using Python interpretable programming language with computationally intensive procedures resolved using efficient compliable libraries at *scipy* with a backend on Fortran and C++ [1].

Charge conservation law can be expressed by the following set of equations [2,3,4]:

$$\frac{d\vec{x}}{dt} = Q\mathbf{A}\vec{x} + \mathbf{J}\vec{x} + I\vec{S}\,, \tag{1}$$

Here $\vec{x} = (x_1, x_2, x_3, x_4, x_5, x_6, x_7, x_8)^T = (c_2^{tk}, c_3^{tk}, c_4^{tk}, c_5^{tk}, c_2^{cell}, c_3^{cell}, c_4^{cell}, c_5^{cell})^T$ is conservations vector,

$$\vec{S} = \left(0, 0, 0, 0, \frac{1}{FV_{cell}}, -\frac{1}{FV_{cell}}, -\frac{1}{FV_{cell}}, \frac{1}{FV_{cell}}\right)^T \tag{2}$$

is a source term representing flux of electrons converting redox species to complementary states in cells,

$$\mathbf{A} = \begin{pmatrix} -\theta & 0 & 0 & 0 & \theta & 0 & 0 & 0 \\ 0 & -\theta & 0 & 0 & 0 & \theta & 0 & 0 \\ 0 & 0 & -\theta & 0 & 0 & 0 & \theta & 0 \\ 0 & 0 & 0 & -\theta & 0 & 0 & 0 & \theta \\ \gamma & 0 & 0 & 0 & -\gamma & 0 & 0 & 0 \\ 0 & \gamma & 0 & 0 & 0 & -\gamma & 0 & 0 \\ 0 & 0 & \gamma & 0 & 0 & 0 & -\gamma & 0 \\ 0 & 0 & 0 & \gamma & 0 & 0 & 0 & -\gamma \end{pmatrix} \tag{3}$$

is a term representing exchange of electrolytes in cells and tanks with $\theta = 1/V_{tk}$ and $\gamma = 1/V_{ce}$, where V_{tk} is the volume of the tank and V_{ce} is the volume o the cell.

CompBat project has received funding from the European Union's Horizon 2020 research and innovation programme under grant agreement No 875565. This document has been produced by the CompBat project. The content in this document represents the views of the authors, and the European Commission has no liability in respect of the content.

$$\mathbf{J} = \begin{pmatrix} 0 & 0 & 0 & 0 & 0 & 0 & 0 & 0 \\ 0 & 0 & 0 & 0 & 0 & 0 & 0 & 0 \\ 0 & 0 & 0 & 0 & 0 & 0 & 0 & 0 \\ 0 & 0 & 0 & 0 & 0 & 0 & 0 & 0 \\ 0 & 0 & 0 & 0 & -J_2 & 0 & -J_4 & -2J_5 \\ 0 & 0 & 0 & 0 & 0 & -J_3 & 2J_4 & 3J_5 \\ 0 & 0 & 0 & 0 & 3J_2 & 2J_3 & -J_4 & 0 \\ 0 & 0 & 0 & 0 & -2J_2 & -J_3 & 0 & -J_5 \end{pmatrix} \quad (4)$$

is a crossover term due to transport of active species across the membrane that also leads to a capacity fading. Taking into account non-linear concentration profiles of redox species in the membrane, the molar flux J_i can be calculated analytically [1]:

$$J_i = \frac{P_i^m c_i^{ce}}{d_m} \frac{\chi_i}{1-\exp(-\chi_i)} \text{ (discharge mode),} \quad (5)$$

$$J_i = \frac{P_i^m c_i^{ce}}{d_m} \frac{\chi_i}{\exp(\chi_i)-1} \text{ (charge mode),} \quad (6)$$

where χ_i is a dimensionless parameter presenting migration and convection:

$$\chi_i = \left(\frac{z_i F}{\sigma^m RT} + \frac{\xi K_i}{P_i^m F \lambda c_f} \right) d_m j^m . \quad (7)$$

The system of equations (1) is numerically solved using adaptive Runge-Kutta method implemented at scipy.integrate library. In order to solve the equation one has, firstly, set initial conditions on organic or vandadium redox species concentrations and, secondly, set time-dependent profiles for current and electrolyte flow rate. While current and flow rates are trivial for calculation, initial states for the system cannot be directly evaluated from the setup and are hidden variables. Moreover, imbalance between tanks complicates the monitoring of concnetrations requring additional measurements such as reference electrode that allows to measure half-cell potentials. In the present approach we assume imbalance to be negligible at the beginning of the battery operation and get concentrations from ideal case, i.e. take values that are believed by experimenters.

CompBat project has received funding from the European Union's Horizon 2020 research and innovation programme under grant agreement No 875565. This document has been produced by the CompBat project. The content in this document represents the views of the authors, and the European Commission has no liability in respect of the content.

Model for battery voltage takes into account the ohmic and mixed concentration and activation losses. The common approach with empirical mass transfer rate constant k_{mt} {cm s^{-1}} was adopted:

$$k_{mt} = \alpha_{mt} u^{\beta_{mt}} \tag{8}$$

Here, α_{mt} and β_{mt} are empirical constants and u {cm s^{-1}} is the electrolyte velocity. The latter is calculated according to (9) from specified electrolyte flow rate Q {l min^{-1}}, the number of cells in the stack N, and electrode geometry for flow-through design, defined by electrode width w {m} and length l {m}:

$$u = \frac{Q}{Nwl} \tag{9}$$

The high carbon felt porosity provides rather low influence on estimated u, which is, in turn, masked by the empirical mass-transfer coefficients. Therefore, it is not considered in (9). The mass-transfer limiting currents for positive I_{lim}^{pe} {A} and negative I_{lim}^{ne} {A} electrolytes can be defined as follows (10):

$$\begin{cases} \begin{bmatrix} I_{lim}^{pe} = FA_{el}k_{mt}c_{pe^R}^{*}, I_{load} > 0 \\ I_{lim}^{pe} = FA_{el}k_{mt}c_{pe^O}^{*}, I_{load} < 0 \end{bmatrix} \\ \begin{bmatrix} I_{lim}^{ne} = FA_{el}k_{mt}c_{pe^O}^{*}, I_{load} > 0 \\ I_{lim}^{ne} = FA_{el}k_{mt}c_{pe^R}^{*}, I_{load} < 0 \end{bmatrix} \end{cases} \tag{10}$$

Here, the positive loading current {A} $I_{load} > 0$ denotes the RFB charging, while the $I_{load} < 0$ is attributed to RFB discharging. F {C mol^{-1}} is Faraday constant, $c_{pe^R}^{*}$, $c_{pe^O}^{*}$, $c_{ne^O}^{*}$, $c_{ne^R}^{*}$ {M} are concentrations of oxidized/reduced vanadium or organic redox species, and A_{el} {m^2} is the electrode surface area. The latter is estimated from a specified surface factor A_f {m^2 m^{-3}} [2] and electrode geometric parameters (w {m}, l {m}, and h {m}) for the carbon felt electrode (11):

$$A_{el} = A_f wlh \tag{11}$$

The open-circuit cell voltage E_{OC} {V} for a single cell in the RFB stack is estimated from the standard potentials of positive E_0^{pe} {V} (12) and negative E_0^{ne} {V} (13) half-cell reactions corrected by activities of redox species and protons (for VRFB) according to the Nernst equation. The activity coefficients were assumed constant at the whole range of SOCs. The constant correction to the open-circuit cell voltage $\Delta E^{soc=50\%}$ was introduced once to account potential drop on the menbrane and non-unit activity coefficients [3]. It is calculated from as the difference between the theoretical and experimental OCV at SOC = 50%. The resulting equation can be represented as follows (14):

CompBat project has received funding from the European Union's Horizon 2020 research and innovation programme under grant agreement No 875565. This document has been produced by the CompBat project. The content in this document represents the views of the authors, and the European Commission has no liability in respect of the content.

$$\begin{cases} E_{eq}^{pe} = E_0^{pe} - \frac{RT}{F} ln\left(\frac{c_{pe^R}^*}{c_{pe^O}^* c_{H^+}^{*\,2}}\right), VFRB \\ E_{eq}^{pe} = E_0^{pe} - \frac{RT}{F} ln\left(\frac{c_{pe^R}^*}{c_{pe^O}^*}\right), ORFB \end{cases} \quad (12)$$

$$E_{eq}^{ne} = E_0^{ne} - \frac{RT}{F} ln\left(\frac{c_{ne^R}^*}{c_{ne^O}^*}\right) \quad (13)$$

$$\begin{cases} E_{OC} = E_{eq}^{pe} - E_{eq}^{ne} = \left(E_0^{pe} - E_0^{ne} + \Delta E^{soc=50\%}\right) - \frac{RT}{F} ln\left(\frac{c_{pe^R}^* c_{ne^O}^*}{c_{pe^O}^* c_{H^+}^{*\,2} c_{ne^R}^*}\right), VRFB \\ E_{OC} = E_{eq}^{pe} - E_{eq}^{ne} = \left(E_0^{pe} - E_0^{ne} + \Delta E^{soc=50\%}\right) - \frac{RT}{F} ln\left(\frac{c_{pe^R}^* c_{ne^O}^*}{c_{pe^O}^* c_{ne^R}^*}\right), ORFB \end{cases} \quad (14)$$

The concentrations in electrolyte bulk were estimated from the state of charge SOC {%} and the total concentration of redox species c^{tot} {M} according to (15):

$$\begin{cases} c_{ne^R}^* = c^{tot} SOC \\ c_{ne^O}^* = c^{tot}(1 - SOC) \\ c_{pe^R}^* = c^{tot}(1 - SOC) \\ c_{pe^O}^* = c^{tot} SOC \end{cases} \quad (15)$$

The sulfuric acid species is assumed to be fully dissociated into H^+ and SO_4^{2-} in VRFB. The reaction rates are calculated within the Butler-Volmer formalism with the notation from Bard and Faulkner [4] for PE and NE as given at (16) and (17) respectively:

$$\begin{cases} r_{a,c}^{pe} = k_{0_{a,c}}^{pe} c_{pe^O} c_{H^+}^{*\,2} exp\left(-\frac{\alpha_{a,c}^{pe} F(E^{pe} - E_0^{pe})}{RT}\right) - k_{0_{a,c}}^{pe} c_{pe^R} exp\left(-\frac{(1-\alpha_{a,c}^{pe}) F(E^{pe} - E_0^{pe})}{RT}\right), VRFB \\ r_{a,c}^{pe} = k_{0_{a,c}}^{pe} c_{pe^O} exp\left(-\frac{\alpha_{a,c}^{pe} F(E^{pe} - E_0^{pe})}{RT}\right) - k_{0_{a,c}}^{pe} c_{pe^R} exp\left(-\frac{(1-\alpha_{a,c}^{pe}) F(E^{pe} - E_0^{pe})}{RT}\right), ORFB \end{cases} \quad (16)$$

$$r_{a,c}^{ne} = k_{0_{a,c}}^{ne} c_{ne^O} exp\left(-\frac{\alpha_{a,c}^{ne} F(E^{ne} - E_0^{ne})}{RT}\right) - k_{0_{a,c}}^{ne} c_{ne^R} exp\left(-\frac{(1-\alpha_{a,c}^{ne}) F(E^{ne} - E_0^{ne})}{RT}\right) \quad (17)$$

Here, c_{pe^O}, c_{pe^R}, c_{ne^O}, and c_{ne^R} {M} are surface concentrations. Generally, they are unknown and different from the concentrations in electrolyte bulk due to mass-transfer effects. Only the surface proton concentration is assumed to be the same because of the higher concentration of sulfuric acid and proton diffusivity in aqueous solutions [5] than that of vanadium species in VRFB at operating conditions. $k_{0_{a,c}}^{pe,ne}$ {PE: VRFB cm s^{-1} M^{-2}, ORFB cm s^{-1}}/{NE: cm s^{-1}} are effective standard rate constants, $\alpha_{a,c}^{pe,ne}$ {-} are charge transfer coefficients. Superscripts *pe* and *ne* go for reactions in posolyte and neolyte respectively, subscripts *a* and *c* imply anodic and cathodic polarization of the half-cell electrode respectively. $E^{pe,ne}$ {V} is the unknown half-cell potential that is to be calculated.

The effective rate constants and charge transfer coefficients are fitted independently within our model for the cathodic and anodic polarization. The difference in these

CompBat project has received funding from the European Union's Horizon 2020 research and innovation programme under grant agreement No 875565. This document has been produced by the CompBat project. The content in this document represents the views of the authors, and the European Commission has no liability in respect of the content.

parameters can be associated with the complex nature of the reaction mechanism (especially, at PE in VRFB [6–9]). The underlying mechanistic complexity is reflected in dependence of identified effective parameters for the simplified single-step mechanism on the operating conditions (e.g. SOC, pH, and the charge/discharge mode). Therefore, the model identification requires the evaluation of model parameters in the range of RFB operating conditions in the manner of lookup table.

The half-cell potentials $E^{pe,ne}$ are obtained from the numerical solution of the system of mass-balance equations (18)-(21) that is solved simultaneously with concentrations of redox species and half-cell potentials.

$$\left(\frac{dc_{pe^O}}{dx}\right)_{x=0} = 0 \approx k_{mt}\left(c^*_{pe^O} - c_{pe^O}\right) - r^{pe}_{a,c} \tag{18}$$

$$\left(\frac{dc_{pe^R}}{dx}\right)_{x=0} = 0 \approx k_{mt}\left(c^*_{pe^R} - c_{pe^R}\right) + r^{pe}_{a,c} \tag{19}$$

$$\left(\frac{dc_{ne^O}}{dx}\right)_{x=0} = 0 \approx k_{mt}\left(c^*_{ne^O} - c_{ne^O}\right) - r^{ne}_{a,c} \tag{20}$$

$$\left(\frac{dc_{ne^R}}{dx}\right)_{x=0} = 0 \approx k_{mt}\left(c^*_{ne^R} - c_{ne^R}\right) + r^{ne}_{a,c} \tag{21}$$

$$\frac{I_{load}}{A_{el}F} + r^{pe}_{a,c} = 0 \tag{22}$$

$$-\frac{I_{load}}{A_{el}F} + r^{ne}_{a,c} = 0 \tag{23}$$

The resulting battery voltage E^{tot}_{bat} with all considered losses is evaluated from (24):

$$\begin{aligned} E^{tot}_{bat} &= N\left(E_{OC} + I_{load}R_{ohm} + \left(E^{pe}_{eq} - E^{pe}\right) + \left(E^{ne}_{eq} - E^{ne}\right)\right) = \\ &= \left(I_{load}R_{ohm} + E^{pe} - E^{ne} + \Delta E^{soc=50\%}\right) \end{aligned} \tag{24}$$

3 Experimental study

Firstly, we validate the model on experimental data obtained at Turku University.

3.1 Test bench

The experimental data was obtained working with a Pinflow standard test cell with the following main parameters:

- Geometrical sizes of electrodes: 40 x 50 x 3.75 mm (after cell compression)
- Membrane area: 20 cm^2
- Cell volume: 6,25 ml

CompBat project has received funding from the European Union's Horizon 2020 research and innovation programme under grant agreement No 875565. This document has been produced by the CompBat project. The content in this document represents the views of the authors, and the European Commission has no liability in respect of the content.

- Number of cells in the stack: 1 cell

The electrodes used in the studied systems were Rayon Graphite Felt BGF5 (6-7 mm thickness), got from CGT Carbon GmbH. The felts were heat treated before usage, kept at 400 °C for 24 hours.

Besides the variables measured in the main cell during the experiments, additional voltage measurements were obtained using extra Pinflow lab cells. The electrolytes flow though the main and secondary cells to come back to the reservoirs. The schema of the system is presented on Fig.1, where the different measurements are listed by digits from 1 to 8.

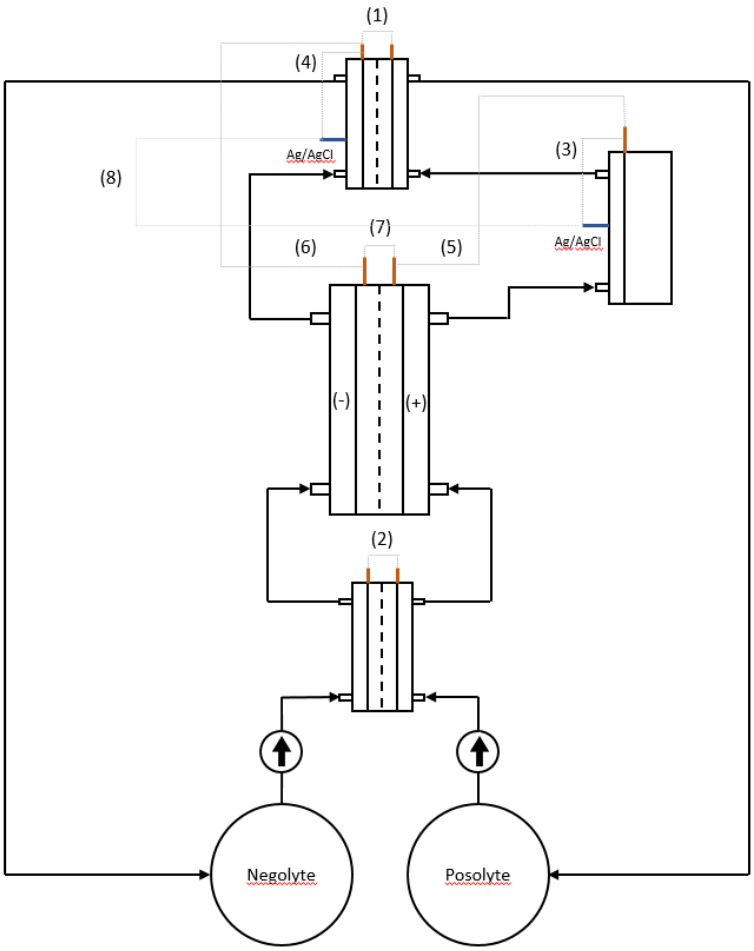

Figure 1: The schema of the experimental test bench.

CompBat project has received funding from the European Union's Horizon 2020 research and innovation programme under grant agreement No 875565. This document has been produced by the CompBat project. The content in this document represents the views of the authors, and the European Commission has no liability in respect of the content.

List of measurements:

1- Open circuit potential after the main cell.
2- Open circuit potential before the main cell.
3- Potential of the Positive Electrode against Reference Electrode Ag/AgCl
4- Potential of the Negative Electrode against Reference Electrode Ag/AgCl
5- Potential of the Positive Electrode after the main cell against the potential of the Positive Electrode in the main cell (Positive Electrode polarization).
6- Potential of the negative Electrode after the main cell against the potential of the Negative Electrode in the main cell (Negative Electrode polarization).
7- Main Cell potential and current density
8- Potential of the Reference Electrode of the Positive side against the Reference Electrode of the Negative side (membrane potential drop).

All the measurements have been performed using a LANHE Battery Testing System G340A (1 channel for each listed measurement). In the case of the Vanadium System, 3 channels were required in the main cell to applied the high currents during the polarization curves (max. current per channel: 5 amps). Additionally, potential electrochemical impedance spectroscopy was performed to obtain the resistance of the main cell using a Biologic SP-240 potentiostat.

All the experiments have been conducted at room temperature (rounded around 25-30 ^{o}C). After each system assembling, the electrolytes were degassed with nitrogen (fed to the reservoir) for at least 1 hour in order to remove the dissolved oxygen. For the Vanadium system, the nitrogen was continuously bubbled into the tanks during the whole experiments. In the case of the organic redox couples, the system was placed into a glove bag in a nitrogen atmosphere.

The polarization curves were measured at 3 different flow rates (0,02, 0,05 and 0,1 l min^{-1}) and 3 different states of charge (20, 50 and 80 %), followed by the charge-discharge curves at constant flow rate (0,1 l min^{-1}) and different current densities. The polarization curves were measured by discharge/charge steps in order to keep constant the state of charge of the battery. In the case of the charge-discharge curves, the applied current for the organic couples was lower than vanadium battery because of the lower concentration of the active species in these systems. The resistance of the system was measured before and after each experiment (both polarization and charge-discharge curves).

3.2 Electrolytes

The electrolytes, the properties and corresponding flow batteries parameters are listed in Table 1.

CompBat project has received funding from the European Union's Horizon 2020 research and innovation programme under grant agreement No 875565. This document has been produced by the CompBat project. The content in this document represents the views of the authors, and the European Commission has no liability in respect of the content.

Table 1. Main properties of the investigated redox couples.

	Vanadium	BTMAP-Fc/Vi	NDI/$Fe(CN)_6$
Tank volume, ml	50	45	50
Cell volume, ml	6.25	6.25	6.25
Ions+conc	V(1.6M), H2SO4(2M)	BTMAP-Fc/ TEMPO-Vi(0.1M), 1M(KCl)	naphtalene diimide/ammonium ferrocyanide (0.1M), NH_4Cl (1M)
Membrane	Nafion 117 (stored in H_2SO_4 2M before assembling)	Selemion DSVN (stored in NaCl 0,25M before assembling)	Sx-053 DK (stored in NH_4Cl 1M before assembling)
Flow rate, ml/min	100 (ch-dc), 20/50/100(pol)	100 (ch-dc), 20/50/100(pol)	100 (ch-dc), 20/50/100(pol)
Voltage	0.9-1.7V	0.3-1.1V	0-0.75V
SOC, %	50	50	50
Voltage model	Ohmic	Ohmic and Concentration	Ohmic and Concentration
Standard potentials	+1.000 V/ -0.255 V	0.375 V/-0.342 V	0.390 V/-0.08;-0.48 V

4 Results and Discussion

The model validation was performed in two steps. On the first step, the polarization curve at SOC = 50% was investigated and used for tuning of the parameters related to simulation of internal losses as Ohmic, activation and concentration. On the second step, the tuned parameters were used for simulation of charge-discharge curves at different loading currents. In addition, the all-vanadium based system was used for model validation as the most stable one. After the organic redox couples have been simulated with prior retuning of the main model parameters.

4.1 Polarization curves modeling

As we mentioned before, we started model validation with all-vanadium based electrolytes as they are the most well-known, the most stable and the most investigated in the literature. The experimental polarization curves show negligible dependence on electrolyte flow rate. Additionally, the experimental cell resistance obtained from EIS is ~30% higher than the extracted from the linear region of polarization curves. This can be due to non-negligible contact resistance. Therefore, instead of decoupling the ohmic, concentration, and activation losses, the simplest model with ohmic losses was used for

CompBat project has received funding from the European Union's Horizon 2020 research and innovation programme under grant agreement No 875565. This document has been produced by the CompBat project. The content in this document represents the views of the authors, and the European Commission has no liability in respect of the content.

the simulations of VRFB polarization curves (no concentration or activation losses explicitly considered). Importantly, the estimated R_{ohm} include all the abovementioned losses which are linearized. The $\Delta E^{soc=50\%}$ is estimated as 67mV from experimental data. The experimental and simulated polarization curve at SOC = 50% for the vanadium system are shown on the fig. 2.

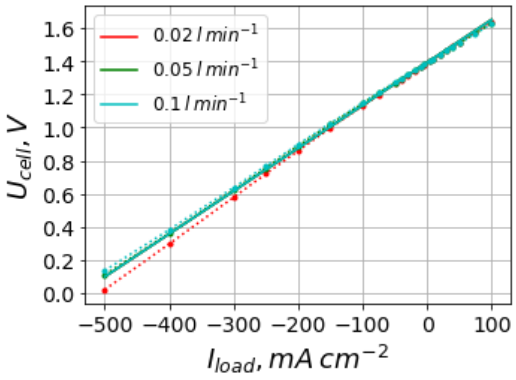

Figure 2: Polarization curve at SOC = 50% for the all-vanadium redox flow system. Experimental results as points with dashed lines and simulation results as solid lines.

The results showed that polarization curves can be accurately reproduced by the voltage model, described above.

After that, the polarization behavior of BTMAP-Vi/BTMAP-Fc, NDI/$Fe(CN)_6$ organic redox couples was investigated (Figure 3 and 4 respectively). As the fast kinetics was observed by Beh et. al [10] for BTMAP-Vi/BTMAP-Fc redox couples, here and further the voltage model with ohmic and concentration losses was applied for this system. For the NDI/$Fe(CN)_6$ system, this model showed good agreement with experiment, hence the fast kinetics was considered by neglecting the activation losses for this couple too. Additionally, for the second redox couple two electron transfer steps occurs at NE side at -0.48 V and -0.08 V vs SHE @standard conditions. Given the standard potential of 0.39 V vs. SHE for PE, the resulting cell voltage was constrained by the low cutoff voltage of 0.75 V to prevent the second electron transfer as it significantly complicates the theoretical treatment of the system. The $\Delta E^{soc=50\%}$ was estimated to be 30 and 66 mV for BTMAP-Vi/BTMAP-Fc and NDI/$Fe(CN)_6$ systems respectively. The fitted parameters are shown at Table 2 and used for all simulations of charge/discharge curves.

CompBat project has received funding from the European Union's Horizon 2020 research and innovation programme under grant agreement No 875565. This document has been produced by the CompBat project. The content in this document represents the views of the authors, and the European Commission has no liability in respect of the content.

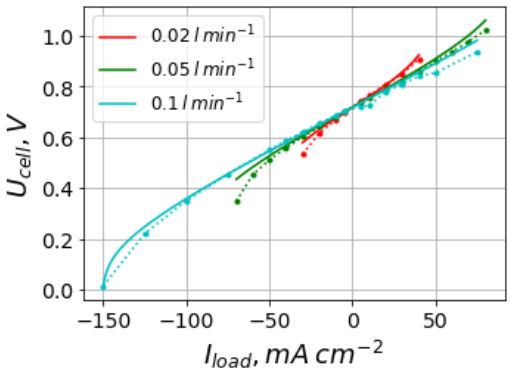

Figure 3: Polarization curve at SOC = 50% for the BTMAP-Vi/Fc system. Experimental results as points with dashed lines and simulation results as solid lines.

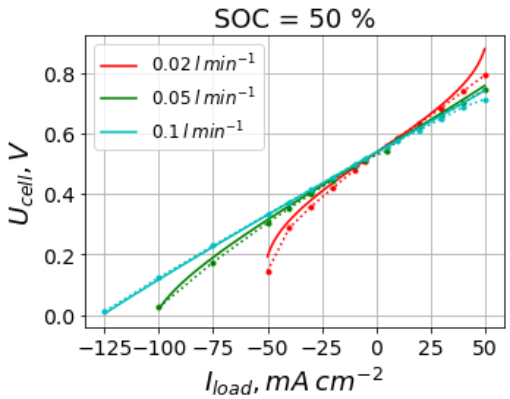

Figure 4: Polarization curve at SOC = 50% for the NDI/$Fe(CN)_6$ system. Experimental results as points with dashed lines and simulation results as solid lines.

Table 2. Fitted voltage model parameters for RFB at SOC = 50%.				
Battery type	R_{ohm}, Ohm	α	β	Fitting Error, MSD
All-Vanadium	0.130	--	--	3.1×10^{-4}
BTMAP-Fc/BTMAP-Vi	0.152	1.4×10^{-4}	0.694	4.6×10^{-4}
NDI/$Fe(CN)_6$	0.189	2.5×10^{-4}	0.777	4.1×10^{-4}

4.2 Simulation of charge-discharge curves

Following the logic of the previous step, first the model was validated for all-vanadium based system. The charge-discharge curves for different galvanostatic loading currents are shown on the Fig 5. Cell area was 20 cm^2.

CompBat project has received funding from the European Union's Horizon 2020 research and innovation programme under grant agreement No 875565. This document has been produced by the CompBat project. The content in this document represents the views of the authors, and the European Commission has no liability in respect of the content.

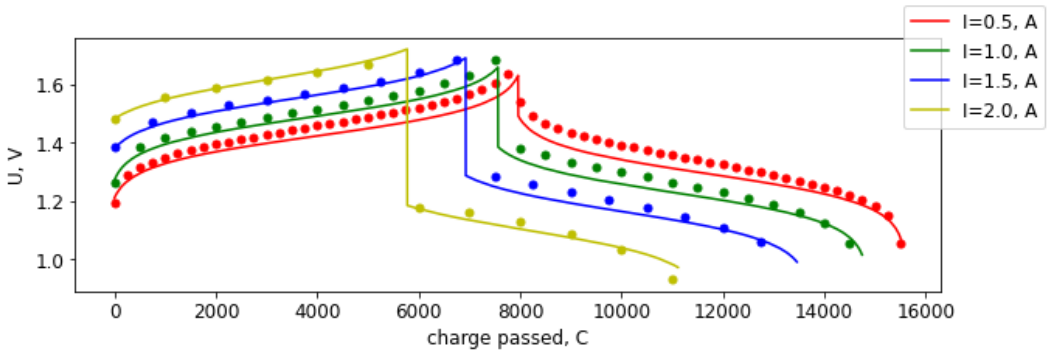

Figure 5: Charge-discharge curves for the all-vanadium system vs. accumulated charge through the battery: dots correspond to measured values, solid lines – to simulated results.

The result showed slight deviations of simulations from the experiments that can be especially noticed at high/low SOC levels. Such difference can be attributed to underestimation of losses by numerical model, which is fitted for moderate SOC.

Nevertheless, the model provides good agreement with experimental data with the average error of 1 %.

The second system is based on BTMAP-Vi/BTMAP-Fc (3-trimethylammonio) propyl-ferrocene dichloride and bis(3-trimethylammonio)propyl viologen tetrachloride aqueous KCl solution. The same setup is used for charge-discharge experiments. At Fig. 6 we compare simulated and experimental voltage (average error ~3%). One can see that in general a moderate agreement is obtained with voltage model including the ohmic and concentration losses. However, from additional experimental half-cell potential studies shown in Appendix A (see fig. A9), where OCV and positive/negative electrolyte potentials are compared, we see obvious imbalance in tanks state of charge: positive half-cell reaches low/high SOC during cycling that is revealed in sharp peaks in the potentials, while negative half-cell potential reveals a smooth evolution, which is the evidence of moderate levels of SOC.

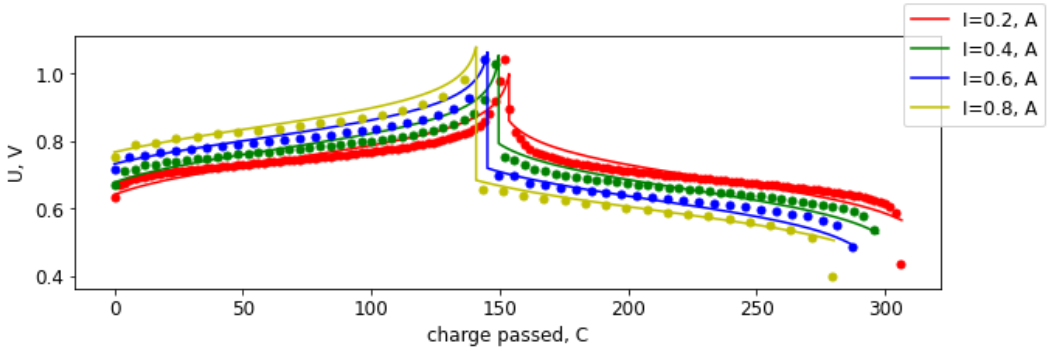

Figure 6: Charge-discharge curves for FcVi system vs. accumulated charge through the battery: dots correspond to measured values, solid lines – to simulated results.

CompBat project has received funding from the European Union's Horizon 2020 research and innovation programme under grant agreement No 875565. This document has been produced by the CompBat project. The content in this document represents the views of the authors, and the European Commission has no liability in respect of the content.

The third system is based on NDI / $Fe(CN)_6$ (0.1M naphtalene diimide/ammonium ferrocyanide in 1M NH4Cl) redox couples. It has the comparable agreement with our model as for the second system (see Fig.7) with average error ~4%.

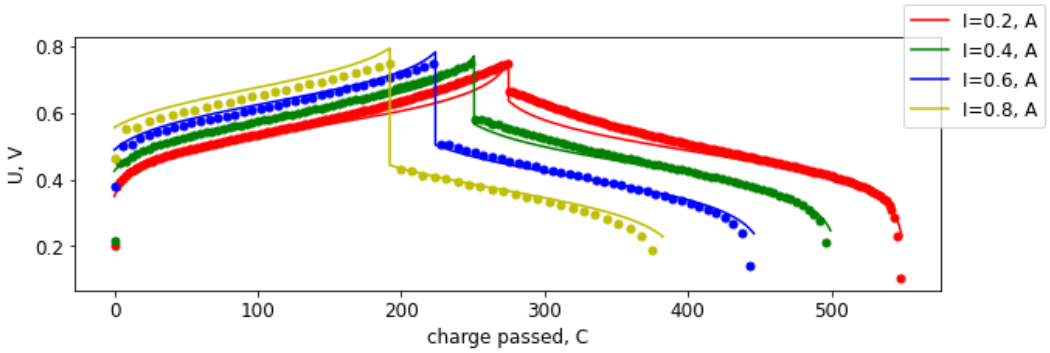

Figure 7: Charge-discharge curves for NDI / $Fe(CN)_6$ system vs. accumulated charge through the battery: 'dots correspond to measured values, solid lines – to simulated results.

The additional studies are performed to elucidate the effect of the lookup table application for the charge/discharge experiment. It is obtained from the voltage model parameters fitted to polarization curves at different SOCs. Additionally, modeling of more diverse experimental dataset with half-cell potentials was studied. However, this part is exceeding the tasks of this project. Therefore, only the preliminary results are shown in the Appendix A which are to be extended in the future work.

4.3 Feasibility analysis of industrial-scale cells performance

In this section the feasibility analysis of polarization behavior and energy performance of industrial-scale cells consisting of 40 cells and with volume of tanks 250L each was performed. In order to do that, the parameters of the cell were modified by the values that correspond to industrial cells (active area approx. 600 cm^2). The simulated polarization curves for all three redox couples are shown on Fig. 8a,b,c.

CompBat project has received funding from the European Union's Horizon 2020 research and innovation programme under grant agreement No 875565. This document has been produced by the CompBat project. The content in this document represents the views of the authors, and the European Commission has no liability in respect of the content.

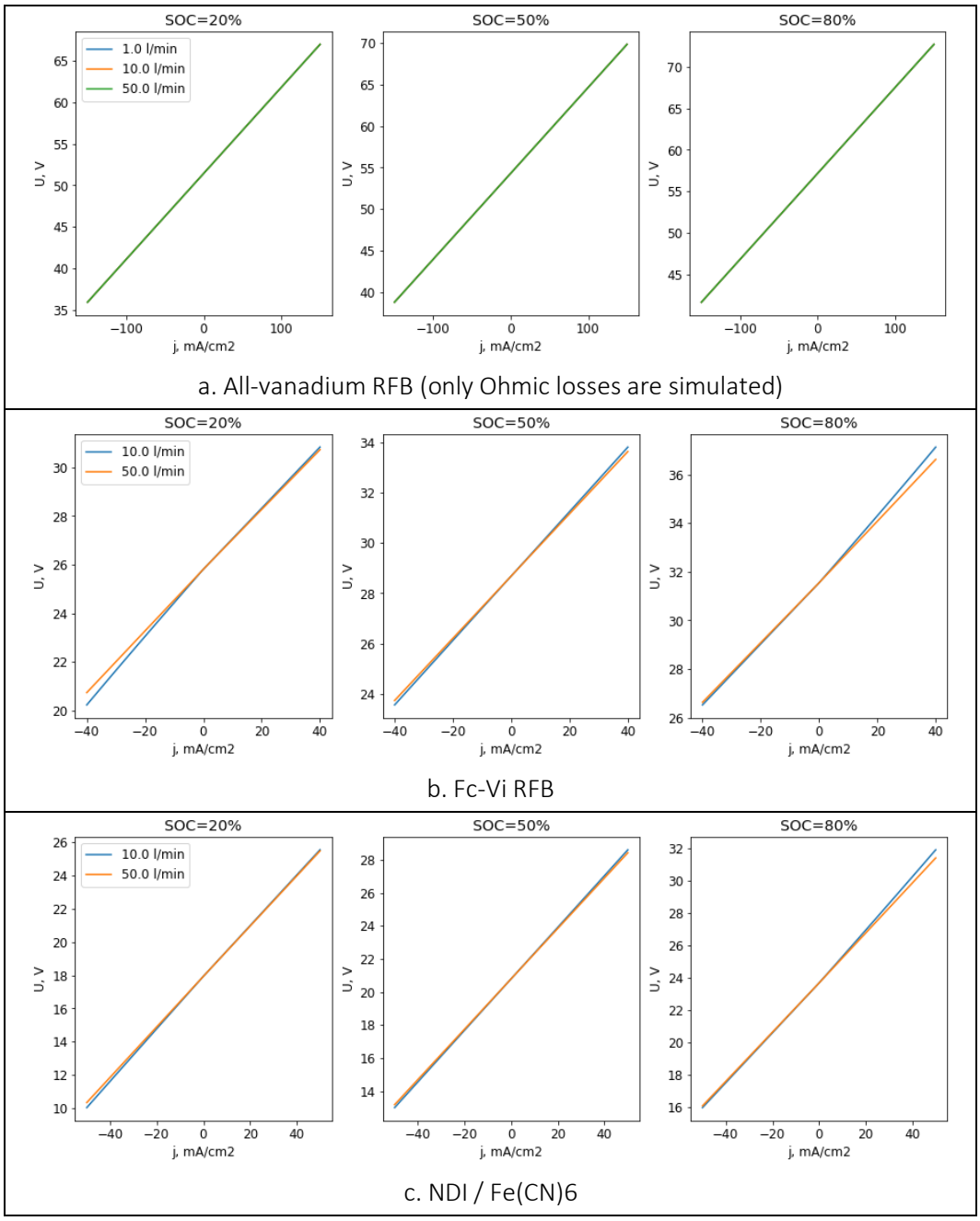

Figure 8: Polarization curves for different redox couples at different flow rates and SOC.

The obtained polarization curves have to be further transferred to UNIPI for Task 3.3.

After that, energy efficiency analysis was performed focusing on the round-trip Coulombic, Voltage and Energy efficiencies as well as on Electrolyte utilization at different loading currents. The obtained results are shown on figures 9a,b,c and 10a,b,c and have to be transferred to UNIPI for application in Task 3.5.

CompBat project has received funding from the European Union's Horizon 2020 research and innovation programme under grant agreement No 875565. This document has been produced by the CompBat project. The content in this document represents the views of the authors, and the European Commission has no liability in respect of the content.

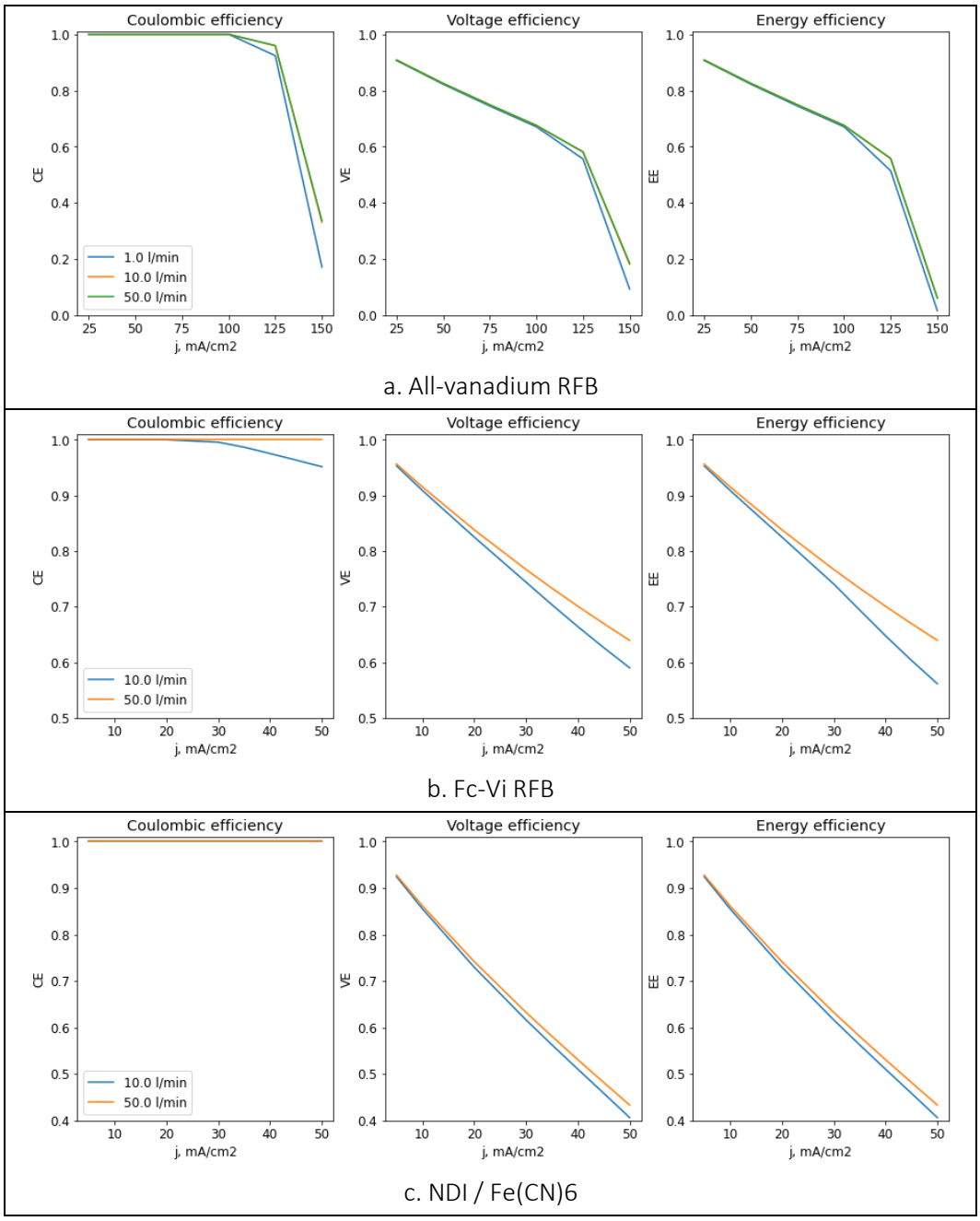

Figure 9: Coulombic, Voltage and Energy efficiencies at different loading currents.

CompBat project has received funding from the European Union's Horizon 2020 research and innovation programme under grant agreement No 875565. This document has been produced by the CompBat project. The content in this document represents the views of the authors, and the European Commission has no liability in respect of the content.

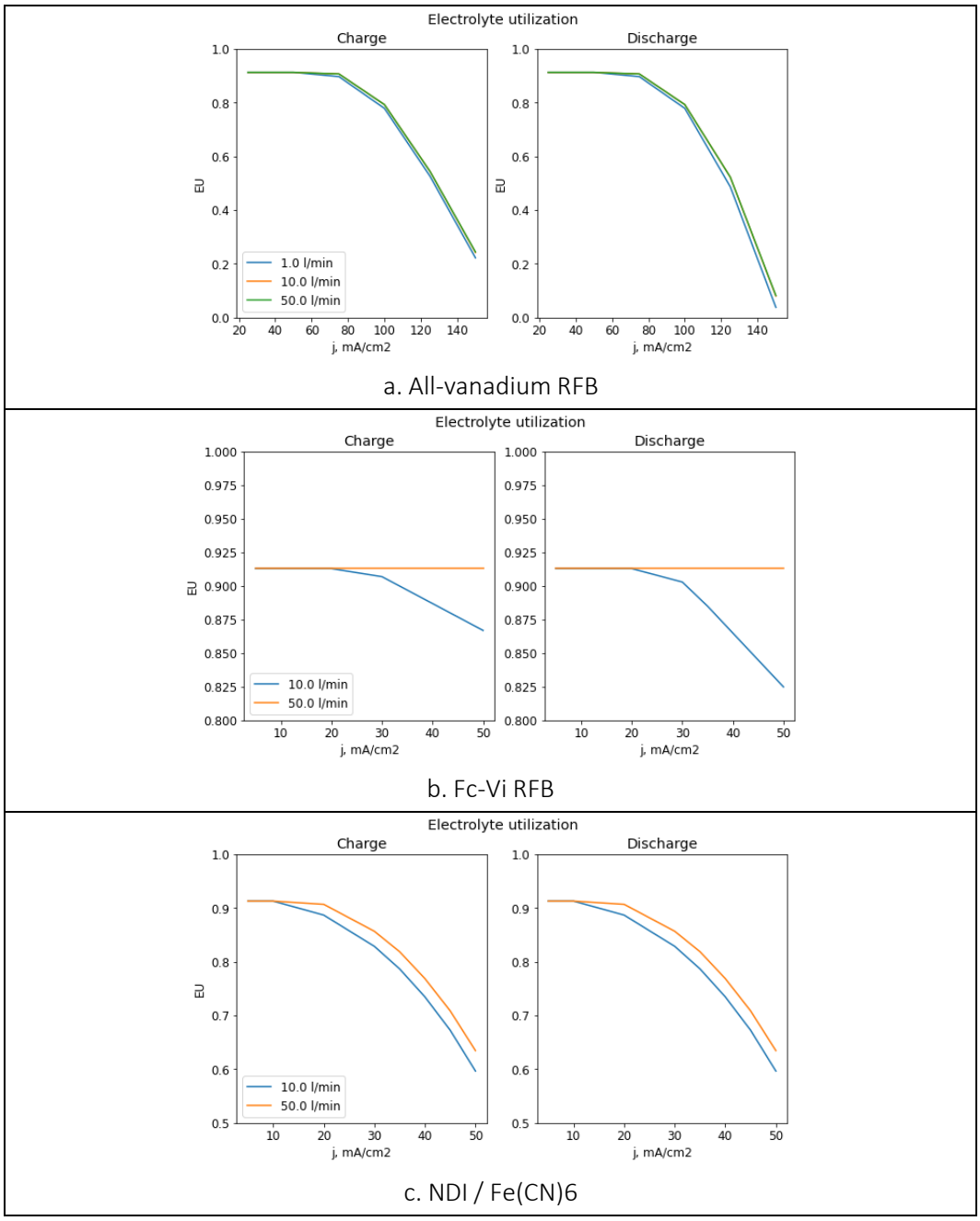

Figure 10: Electrolyte utilization at different loading currents.

5 Conclusions

We derived and implemented a zero-dimensional (0D) model for RFB simulation. The model is based on charge conservation laws and takes into account:

- Nernst potential due to ions concentrations difference,

CompBat project has received funding from the European Union's Horizon 2020 research and innovation programme under grant agreement No 875565. This document has been produced by the CompBat project. The content in this document represents the views of the authors, and the European Commission has no liability in respect of the content.

- Ohmic losses due to electrical resistivity of a cell,
- concentration losses based on concentration profiles near electrodes,
- activation losses due to different kinetics of Redox couples,
- ions exchange between cells and tanks,
- ions exchange between half-cells.

We tuned the voltage model on polarization curves and then validate the total model on charge-discharge voltage data on different current densities on the following Redox couples provided by the project partners:

- All-vanadium RFB,
- Fc-Vi based RFB,
- NDI / Fe(CN)6 based RFB.

We show that the developed 0D model allows simulation of RFB operation with high fidelity (root mean square between simulated and experimental data for all the cases simulated is less than 5%). We also show that the approach allows for evaluation of an industrial-scale RFB. Further research should be devoted to, firstly, model extension to non-isothermal case and, secondly, to its adaptation for capacity fading simulation.

6 References

[1] https://github.com/SoulDancer27/RFB-modeling

[2] Pugach M, Vyshinsky V, Bischi A. Energy efficiency analysis for a kilo-watt class vanadium redox flow battery system. Appl Energy 2019;253:113533. doi:10.1016/j.apenergy.2019.113533.

[3] Pugach M, Kondratenko M, Briola S, Bischi A. Zero dimensional dynamic model of vanadium redox flow battery cell incorporating all modes of vanadium ions crossover. Appl Energy 2018;226:560–9. doi:10.1016/j.apenergy.2018.05.124.

[4] Pugach M, Kondratenko M, Briola S, Bischi A. Numerical and experimental study of the flow-by cell for Vanadium Redox Batteries. Energy Procedia 2017;142:3667–74. doi:10.1016/j.egypro.2017.12.260.

[5] R.M. Darling, A.Z. Weber, M.C. Tucker, M.L. Perry, The Influence of Electric Field on Crossover in Redox-Flow Batteries, J. Electrochem. Soc. 163 (2016) A5014–A5022. https://doi.org/10.1149/2.0031601jes.

[6] Darling RM, Weber AZ, Tucker MC, Perry ML. The Influence of Electric Field on Crossover in Redox-Flow Batteries. J Electrochem Soc 2016;163:A5014–22. https://doi.org/10.1149/2.0031601jes.

CompBat project has received funding from the European Union's Horizon 2020 research and innovation programme under grant agreement No 875565. This document has been produced by the CompBat project. The content in this document represents the views of the authors, and the European Commission has no liability in respect of the content.

[7] Moro F, Trovò A, Bortolin S, Del Col D, Guarnieri M. An alternative low-loss stack topology for vanadium redox flow battery: Comparative assessment. J Power Sources 2017;340:229–41. https://doi.org/10.1016/j.jpowsour.2016.11.042.

[8] Knehr KW, Kumbur EC. Open circuit voltage of vanadium redox flow batteries: Discrepancy between models and experiments. Electrochem Commun 2011;13:342–5. https://doi.org/10.1016/j.elecom.2011.01.020.

[9] Bard AJ, Faulkner LR, Swain E, Robey C. Fundamentals and Applications. n.d.

[10] Beh ES, De Porcellinis D, Gracia RL, Xia KT, Gordon RG, Aziz MJ. A Neutral pH Aqueous Organic–Organometallic Redox Flow Battery with Extremely High Capacity Retention. ACS Energy Lett 2017;2:639–44. https://doi.org/10.1021/acsenergylett.7b00019.

[11] Gvozdik NA, Stevenson KJ. In situ spectroelectrochemical Raman studies of vanadyl-ion oxidation mechanisms on carbon paper electrodes for vanadium flow batteries. Electrochim Acta 2021;383:138300. https://doi.org/10.1016/j.electacta.2021.138300.

[12] Gattrell M, Park J, MacDougall B, Apte J, McCarthy S, Wu CW. Study of the Mechanism of the Vanadium 4+/5+ Redox Reaction in Acidic Solutions. J Electrochem Soc 2004;151:A123. https://doi.org/10.1149/1.1630594.

[13] Gattrell M, Qian J, Stewart C, Graham P, MacDougall B. The electrochemical reduction of VO2+ in acidic solution at high overpotentials. Electrochim Acta 2005;51:395–407. https://doi.org/10.1016/j.electacta.2005.05.001.

[14] Wang W, Fan X, Liu J, Yan C, Zeng C. A novel mechanism for the oxidation reaction of VO2+ on a graphite electrode in acidic solutions. J Power Sources 2014;261:212–20. https://doi.org/10.1016/j.jpowsour.2014.03.053.

CompBat project has received funding from the European Union's Horizon 2020 research and innovation programme under grant agreement No 875565. This document has been produced by the CompBat project. The content in this document represents the views of the authors, and the European Commission has no liability in respect of the content.

Appendix A

1) VRFB

The extended dataset for the VRFB polarization curves at SOC = 20, 50, 80% (Fig. A1) was used to fit the parameters for voltage model with Ohmic losses. The results (Table A1) are further used as the lookup table in charge/discharge experiments.

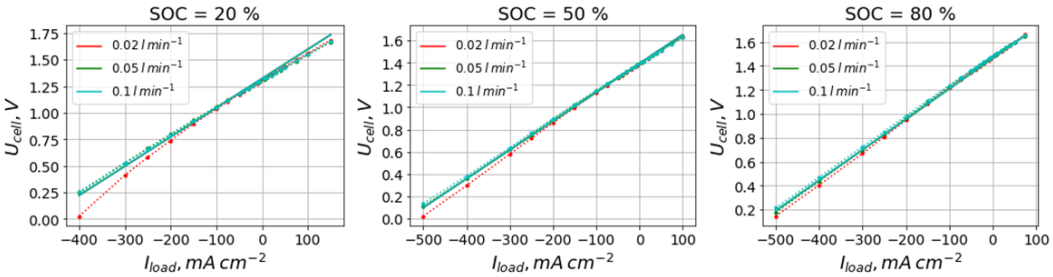

Figure A1: Polarization curves for the all-vanadium redox flow battery. Experimental results as points with dashed lines and simulation results as solid lines.

Table A1. Fitted voltage model parameters for VRFB.		
SOC, %	R_{Ohm}, Ohm	MSD
20	0.138	1.4e-3
50	0.130	3.1e-4
80	0.127	3.3e-4

The validation with data from OCV cells and Ref. electrodes has been performed (Fig. A3). Here one can see quite good agreement with theoretical estimations. Note also that NE potential is corrected to +0.18 V. Moreover, the simulation and experiment fit well for OCV, however, half-cell potentials provide a bit worse results. Possible reasons for the difference can be attributed to different flow topologies in OCV cell and half-cells. In particular, if an flow frame has parts where the electrolyte is not well-fed, i.e. stagnated zones, that leads to different effective electrolyte concentration and hence potential.

CompBat project has received funding from the European Union's Horizon 2020 research and innovation programme under grant agreement No 875565. This document has been produced by the CompBat project. The content in this document represents the views of the authors, and the European Commission has no liability in respect of the content.

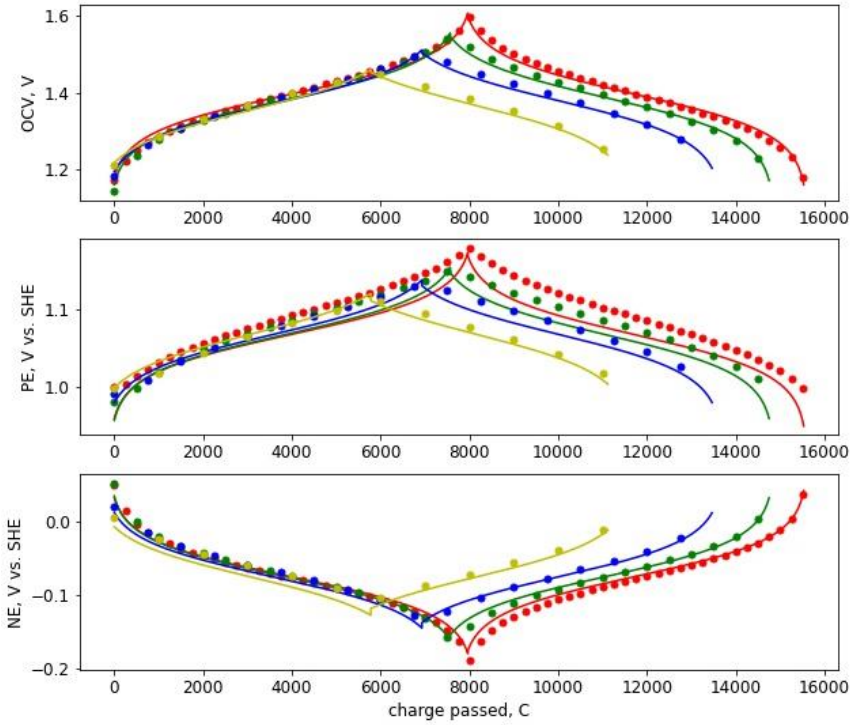

Figure A2: OCV, posilyte and negolyte potentials for the all-vanadium system: dots correspond to experimental solid – to simulated data. Note that simulated NE potential is shifted by -0.2 V and PE potential – to -0.03 V in order to obtain qualitative agreement.

2) BTMAP-Fc/BTMAP-Vi

The modeling of experimental data for BTMAP-Fc/BTMAP-Vi system faced some limitations as the electrolyte imbalance was observed in experimental data (Fig A5). The SOCs at 20% and 80% was changed to 30% and 70% to mimic it. The OCV was corrected accordingly (Fig. A3). Still, the results (Fig. A4) should be used with care only to try the extended simulation approach with the lookup table for estimated parameters. Final results are to be obtained after the further experimental study.

CompBat project has received funding from the European Union's Horizon 2020 research and innovation programme under grant agreement No 875565. This document has been produced by the CompBat project. The content in this document represents the views of the authors, and the European Commission has no liability in respect of the content.

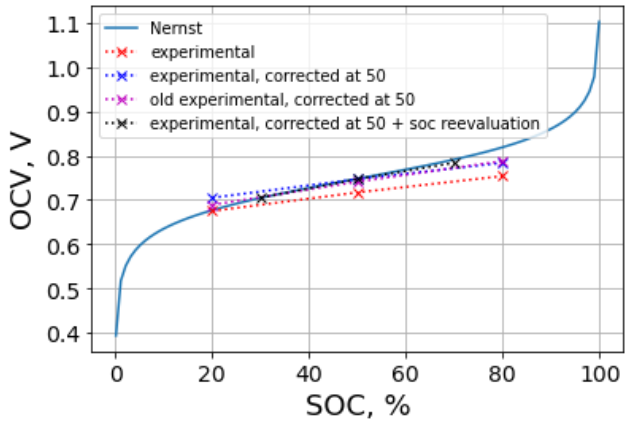

Figure A3: Theoretical and experimental OCV. The values from Nernst equation (solid blue line), the experimental OCV (dashed red line), experimental OCV with the corrections at SOC=50% (dashed blue line), and SOC-corrected experimental OCV (dashed black line) are shown.

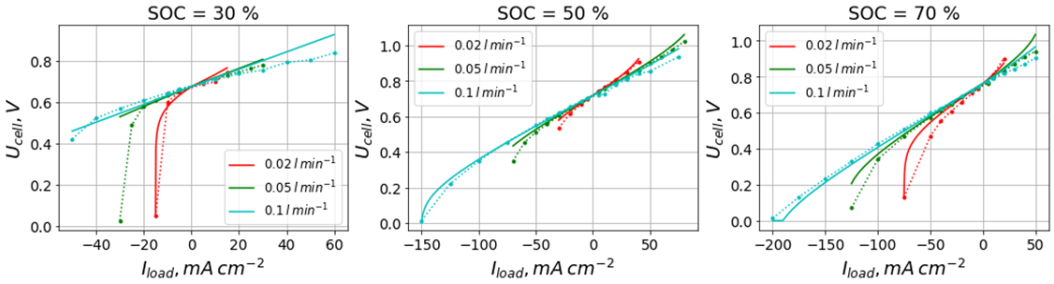

Figure A4: Polarization curves for the BTMAP-Fc/BTMAP-Vi organic redox flow battery. Experimental results as points with dashed lines and simulation results as solid lines.

CompBat project has received funding from the European Union's Horizon 2020 research and innovation programme under grant agreement No 875565. This document has been produced by the CompBat project. The content in this document represents the views of the authors, and the European Commission has no liability in respect of the content.

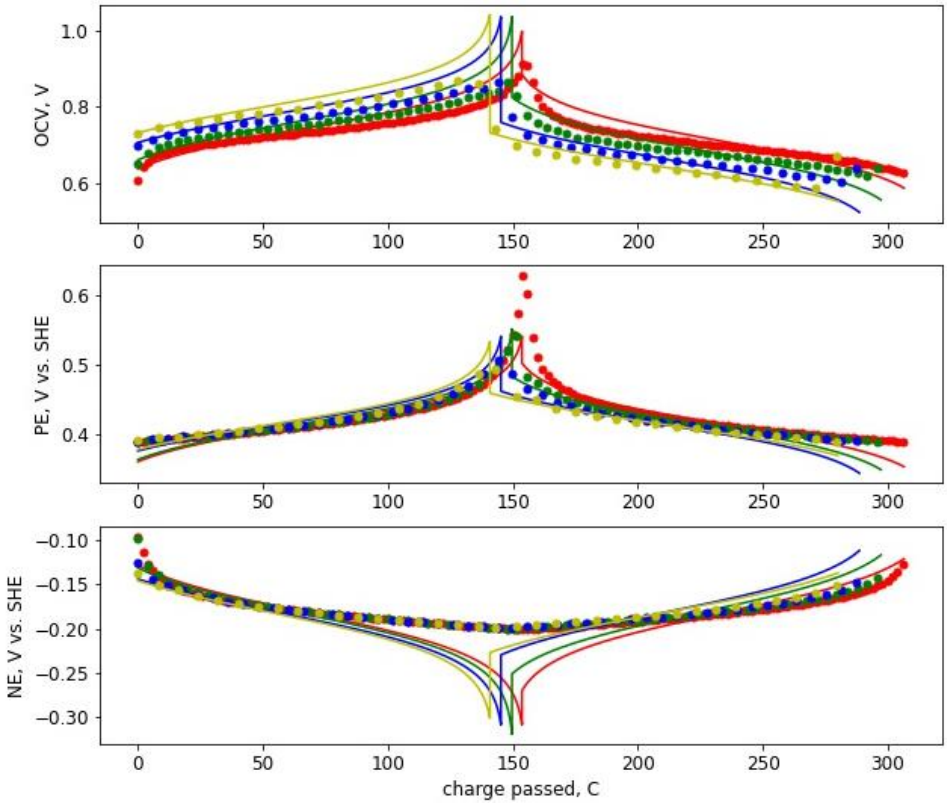

Figure A5: OCV, posilyte and negolyte potentials for BTMAP-Fc/BTMAP-Vi system: dots correspond to experimental solid – to simulated data.

More interesting is the analysis of measured OCV and half-cells potential. Note here that PE potential is corrected by 55mV and NE potential to 145mV. Firstly, we see that simulation fails to properly fit experimental OCV both in OCV mean angle and extrema (Fig. A3). The reason becomes evident when we look at half-cells potential: when PE starts to significantly growth in the middle of the graph, that is the result of high PE SOC, NE is at its linear phase, i.e. at moderate SOC levels. Thus, the observed behavior is the result of SOC imbalance between half-tanks. It is worth noticing here that polarization curves obtained in experiments are assumed to be measured without the imbalance and thus an optimization procedure for the voltage model identification is made for the SOC provided, i.e. without an imbalance. That definitely cause errors in the voltage model. In order to mitigate these errors one should measure SOC values for PE and NE independently and include the information in polarization plots data.

3) NDI/$Fe(CN)_6$

The third redox couple NDI/$Fe(CN)_6$ is also processed. Here we had to correct OCV in order to fit experimental data by an equilibrium potential shift at SOC 50% (see fig. A6, A7). Still, the experimental OCVs different at SOC 80% from the estimated within Nernst equation and corrections. Possibly the $2e^-$ reduced NE redox species start to influence the

CompBat project has received funding from the European Union's Horizon 2020 research and innovation programme under grant agreement No 875565. This document has been produced by the CompBat project. The content in this document represents the views of the authors, and the European Commission has no liability in respect of the content.

equilibrium potential at high SOCs (fig. A7). Therefore, the parameters for the polarization curve at SOC 80% were not used for charge/discharge simulations (see fig. A8).

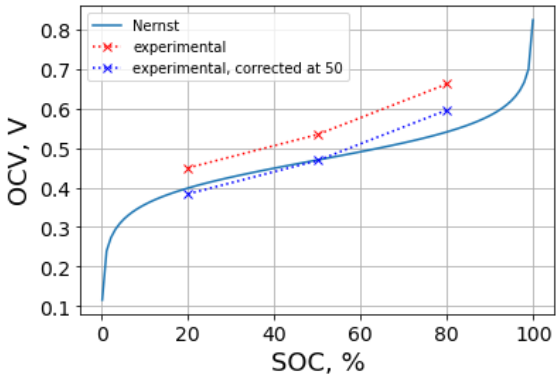

Figure A6: Theoretical and experimental OCV for NDI/$Fe(CN)_6$ system. The values from Nernst equation (solid blue line), the experimental OCV (dashed red line), experimental OCV with the corrections at SOC=50% (dashed blue line) are shown.

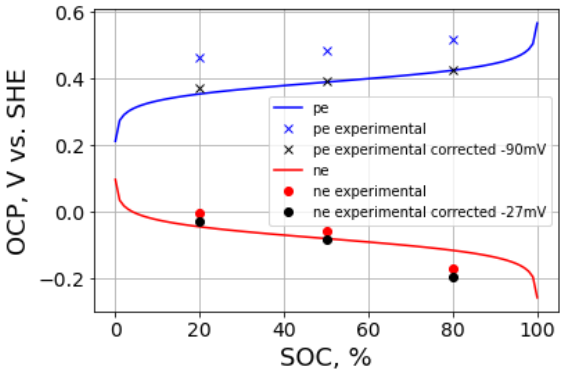

Figure A7: Theoretical and experimental OCP for PE and NE of NDI/$Fe(CN)_6$ system.

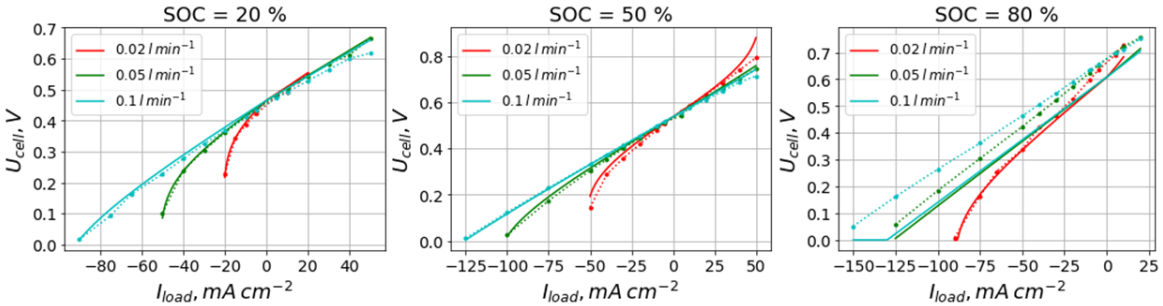

Figure A8: Polarization curves for the NDI/$Fe(CN)_6$ organic redox flow battery. Experimental results as points with dashed lines and simulation results as solid lines.

CompBat project has received funding from the European Union's Horizon 2020 research and innovation programme under grant agreement No 875565. This document has been produced by the CompBat project. The content in this document represents the views of the authors, and the European Commission has no liability in respect of the content.

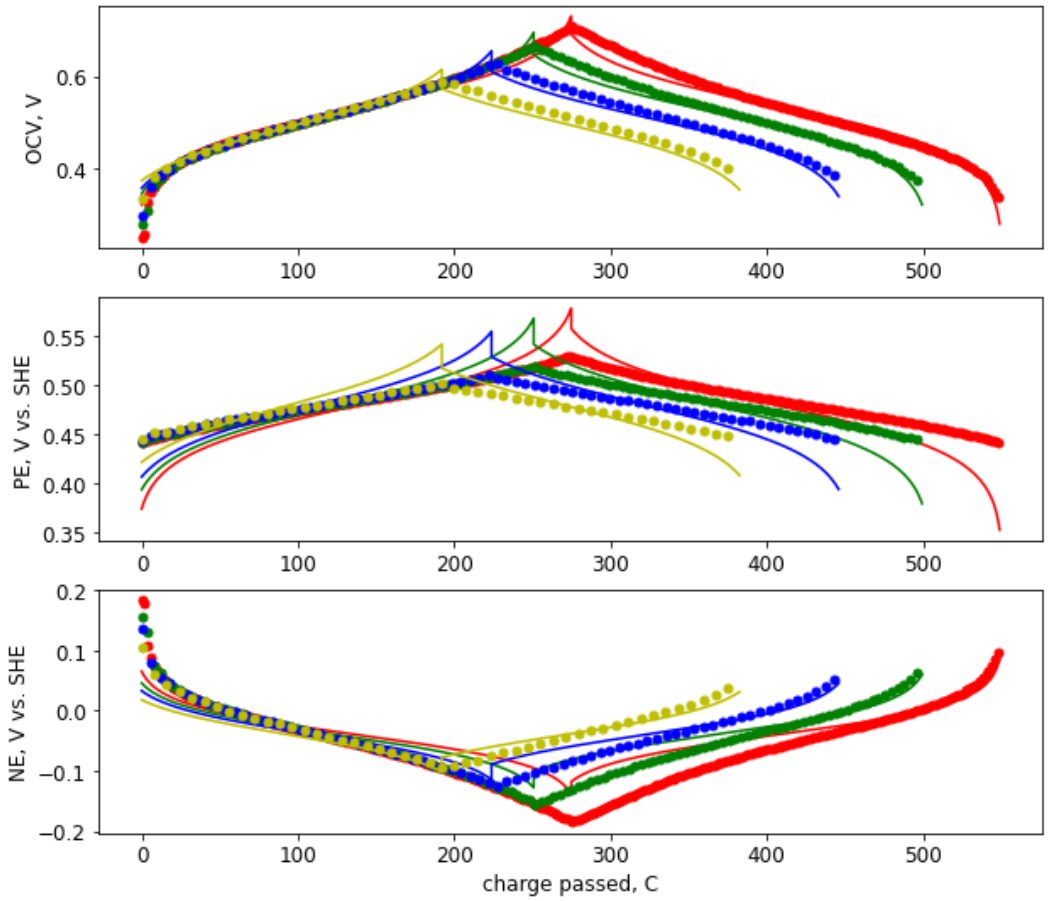

Figure A9: OCV, posilyte and negolyte potentials for NDI / $Fe(CN)_6$ system: dots correspond to experimental solid – to simulated data.

Experimental and simulated OCV fits well (see Fig. A9), while half-cells potentials differ more significantly. PE and NE potentials are corrected by +40mV. One can see that NE potential during cycling work in moderate SOC range, i.e. without significant losses, while PE displays more noticeable peaks. It can be attributed to different capacitances of positive and negative tanks, or the involvement of second electron transfer step at NE. In order to address these issues, additional experiments need to be conducted.

CompBat project has received funding from the European Union's Horizon 2020 research and innovation programme under grant agreement No 875565. This document has been produced by the CompBat project. The content in this document represents the views of the authors, and the European Commission has no liability in respect of the content.